

Venturi Meter Performance on Tee Branch with Converging Run Flow

E. Elliot Naulu*, Michael C. Johnson**, Zachary B. Sharp***

*Department of Civil and Environmental Engineering, Utah State University, Logan Utah

Email: elliottnaulu@gmail.com

**Department of Civil and Environmental Engineering, Utah State University, Logan Utah

Email: michael.johnson@usu.edu

***Department of Civil and Environmental Engineering, Utah State University, Logan Utah

Email: zachary.sharp@usu.edu

Abstract:

Venturi flow meters are often installed downstream of pipe fittings that cause disturbances in the flow profile that may cause inaccurate flow measurement. One such installation is on the branch of a tee junction with converging run flow. Under these conditions, laboratory calibration may be needed to validate the Venturi meter's performance so that accurate metering is achieved. However, in some cases laboratory calibration may not be possible. For this reason, this research used physical testing coupled with computational fluid dynamics (CFD) to determine adjustments to the discharge coefficient for a series of tee installations. The discharge coefficients from the tee installations were divided by straight-line discharge coefficients of identical Reynolds number to create a ratio to adjust the straight-line discharge coefficient and more accurately measure the flow rate in the tee installation.

Keywords —Venturi, Tee Junction, CFD, Discharge Coefficient.

I. INTRODUCTION

Flow measurement is an essential parameter in many processes. For this reason, a substantial amount of research has been geared towards determining the required pipe diameters needed between pipe fittings and the Venturi meter. For example, The American Society of Mechanical Engineers (ASME) provided a range of 8 to 16 diameters for a classical Venturi meter installed downstream of a single 90-degree elbow, with the range being relative to the meter's beta ratio. The beta ratio is defined as the ratio between the Venturi meter's throat diameter to the inlet diameter (Figure 1).

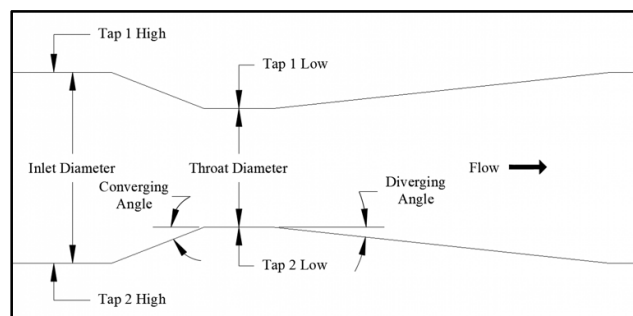


Fig. 1 Plan view of general geometry of a Classical Venturi meter

While a Venturi meter is most accurate when installed per the manufacturer's guidelines or published codes, it is not uncommon for Venturi meters to be installed in less than ideal conditions. When this occurs, the flow profile is disturbed, and the design discharge coefficient may no longer

produce an accurate flow measurement. To achieve accurate flow measurement, The Venturi meter would need to be calibrated in a laboratory with the same or very similar pipe configuration as the field installation. The laboratory calibration would produce a new discharge coefficient that would properly represent the disturbed flow profile from the disturbance upstream. One such installation is a Venturi meter installed on the branch of a tee junction with converging run flow (Figure 2).

The results of this study will illustrate CFD's ability to model a Venturi meter when installed in such an application.

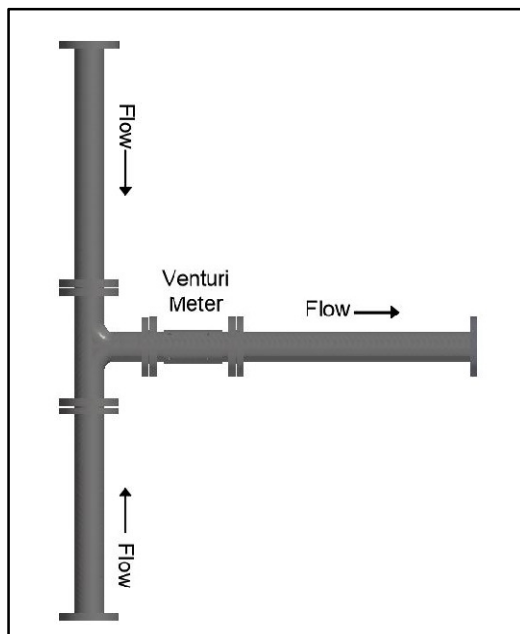


Fig. 2 Sketch of flow through Venturi meter

II. LITERATURE REVIEW

A thorough literature review was conducted to understand what others have presented on the topic. While no literature was found regarding the proposed research topic of converging flow in a tee junction and its effects on the accuracy of a Venturi meter, considerable research exists on pressure losses through tee junctions and Venturi meter performance with flow disturbances upstream.

ASME MFC-3M is a standard used to provide guidance on the proper installation of differential

pressure flowmeters such as orifice plates, classical Venturi meters, and nozzles [1]. While the standard does not provide a minimum distance downstream of a tee-junction for a classical Venturi meter installation, the standard does provide the minimum distance for a single 90-degree elbow, which is between 8 and 16 diameters.

Costa and colleagues compared a sharp-edged tee to a rounded tee and how their geometries influence the pressure profile [2]. They examined the flow characteristics of both the straight flow and the branched flow to develop a loss coefficient. They observed that the rounded tee generated more turbulence in the branch pipe, which resulted in a weaker and shorter recirculation bubble region and consequently a lower loss coefficient.

Abdulwahhab and colleagues investigated how the $k-\epsilon$ turbulence model predicted pressure losses in a tee junction [3]. They analyzed the effect different area ratios of the inlets had on the pressure field and found that as the branch area decreases the velocity increases and consequently generates more recirculation and turbulence. As expected, they concluded that higher pressure loss coefficients were a direct result of higher flow rates.

Sharp studied the energy losses that occur in crosses. He developed energy loss coefficients (K-factors) for four different flow scenarios [4]. The flow scenario that most closely resembled the proposed research was his combining flow scenario, this scenario had converging flow in the three of the four legs with the other leg being the outlet. Sharp found that the K-factors were higher in the combining flow scenario when the leg perpendicular to the outlet leg passed majority of the flow, creating a vortex in the pipe and consequently a significant amount of energy loss.

Stauffer researched how using a hydraulic average of multiple tap sets would improve the accuracy of a Venturi flowmeter when installed downstream of a disturbance [5]. The disturbances upstream of the Venturi flowmeter included a short radius elbow and a butterfly valve set at both full open and 45 degrees open. Stauffer found that the uncertainty in the flow measurement decreased by

half when using a hydraulic average of multiple tap sets.

Sandberg investigated CFD's competency in predicting flow measurement for a Venturi flowmeter installed on the branch of a tee junction with flow passing through the run [6]. Sandberg tested different types of tees (sharp versus smooth), Venturi geometries (classical versus UVT), and distances downstream of the tee (0D, 2D, 5D, 10D). Sandberg found that the classical Venturi geometry yielded a more predictable deviation from the straight trend than the UVT geometry. Sandberg concluded that CFD effectively simulated the majority of the physical data with the exception of the low flow splits.

Day researched the accuracy of a Venturi flowmeter installed downstream of the through leg of a tee junction [7]. Day found that the accuracy of the flowmeter was greatly affected as the flow split between the branch and through leg of the tee. The accuracy increased as a greater ratio of the flow was directed through the flowmeter.

The research presented in this literature review is related in that most articles focus on the improvement of flow measurement. This topic is unique because it focuses on CFD's ability to simulate physical data where there is converging flow in the run of the tee junction. The research will be beneficial to flowmeter users due to the complete lack of published research that exists on single-phase converging flow metered adjacent to a tee junction.

III. METHOD

The physical laboratory data for this research was conducted at the Utah Water Research Laboratory (UWRL) in Logan, Utah. The model consisted of a 6-in Universal Venturi Tube (UVT) with a beta ratio of 0.7 and a 6-inch rounded-corner tee junction. A straight-line test was conducted to illustrate how the UVT meter performed under ideal conditions, and a series of zero-diameter (0D) and five-diameter (5D) runs followed. Differential pressure, flow, and temperature were measured to determine C , and the uncertainty in the results were

determined following the ASME PTC 19.1.2005 test uncertainty national standard [8].

Due to the anticipated turbulence created from the converging flow in this research, four pressure tap sets were considered for both the physical testing and the CFD models (Figure 3). Each tap set consists of a high tap located on the meter's inlet and a low tap on the meter's throat. The four tap sets provided insight into understanding the flow profile and the impacts the converging flow has on the Venturi meter.

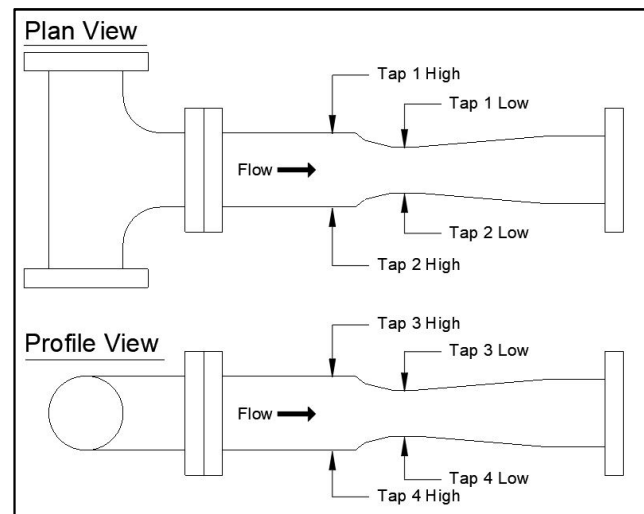


Fig. 3 Tap set configurations

The Venturi equation is used to calculate the discharge coefficient, C , which is a ratio of the actual flow rate to the theoretical flow rate. The discharge coefficient accounts for the small amount of head loss that occurs throughout the Venturi meter due to wall and fluid friction. Assuming a volumetric flow rate and no thermal expansion effects, the Venturi equation for an incompressible fluid becomes:

$$Q = C * A_t * \sqrt{\frac{2 * g_c * \Delta P}{(1 - \beta^4) * \rho_f}}$$

Where:

Q = flow rate, $\frac{ft^3}{s}$

C = discharge coefficient

A_t = area of the throat, ft^2

g_c = gravity constant, $32.17405 \frac{\text{ft}}{\text{s}^2}$

ΔP = differential pressure, $\frac{\text{lb}}{\text{ft}^2}$

β = beta ratio

ρ_f = density of fluid, $\frac{\text{lb}}{\text{ft}^3}$

The straight-line test acted as a benchmark for the 0D and 5D tests. The straight-line installation had 14 feet of upstream pipe, which was considered sufficient to allow for a developed and uniform flow profile to form (Figure 4). The test consisted of eight data points ranging in Reynolds numbers from 71,000 to 793,000.

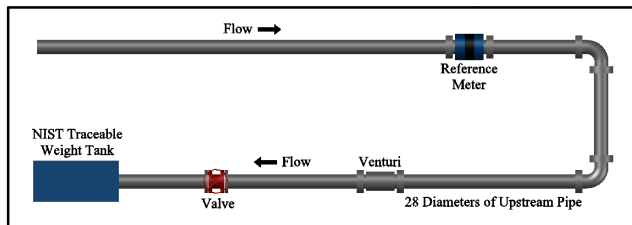


Fig. 4 Straight-line installation

The 0D and 5D test setup consisted of converging lines and connected at a tee junction with the Venturi meter installed on the branch (Figure 5). The 0D and 5D tests required two reference meters, one on the outlet to measure total flow and the other on one of the two converging flows. The non-metered line flow was found by simply subtracting the metered line flow from the total flow. To ensure that the flow profiles entering the tee junction from the converging lines were fully developed and uniform, flow straighteners were installed in each line downstream of the elbows. The 0D and 5D tests consisted of three flows (1800, 1200, 400 gpm), with each flow having four runs or flow splits (Table I).

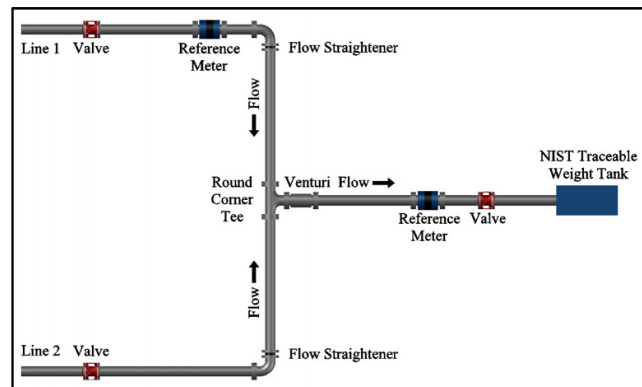


Fig. 5 General flow configuration

TABLE I
FLOW SPLITS

1800 gpm		
Run (Flow Split)	Line 1 (gpm)	Line 2 (gpm)
Run 1 (100/0)	1800	0
Run 2 (80/20)	1440	360
Run 3 (60/40)	1080	720
Run 4 (0/100)	0	1800
1200 gpm		
Run (Flow Split)	Line 1 (gpm)	Line 2 (gpm)
Run 1 (100/0)	1200	0
Run 2 (80/20)	960	240
Run 3 (60/40)	720	480
Run 4 (0/100)	0	1200
400 gpm		
Run (Flow Split)	Line 1 (gpm)	Line 2 (gpm)
Run 1 (100/0)	400	0
Run 2 (80/20)	320	80
Run 3 (60/40)	240	160
Run 4 (0/100)	0	400

The CFD modelling for this research was performed at the UWRL. CFD is a numerical modelling method used to analyze fluid flow and has been used in practice since the 1960's. It is a method that has grown in relevance and has proven quantitatively its ability to predict the performance of flowmeters [9]. One of the many strengths of CFD is the ability to manipulate elements of the model that would otherwise be time consuming, expensive, and difficult to achieve in physical modelling. The

purpose of CFD in this work is not to replicate the absolute values of the physical models, but rather to replicate the percent change from the straight-line test of the respective methods as one of CFD's key strengths is its capability to identify differences from one configuration to another.

CFD is capable of using different turbulence models to generate a solution. Some of these turbulence models include Reynolds-Averaged Navier Stokes (RANS), Detached Eddy, and Large Eddy. The physics models used in this research included: three-dimensional space, steady state, liquid material, segregated flow, gradients, constant density, turbulent regime, RANS model, K-Epsilon turbulence model, two-layer all y + wall treatment, realizable K-Epsilon two-layer, and exact wall distance.

Essential to any CFD model is its mesh or grid. In order to analyze fluid flow numerically, the system is divided into small cells (Figure 6). Each cell passes information to the next making the transition from cell to cell essential. An inaccurate mesh can lead to extensive run times or a solution that does not converge on an accurate numerical solution. While the number of prism layers, prism layer stretching, and the prism layer thickness were adjusted to achieve the most accurate results, the same base cell size was used for all 6-inch simulations. The meshing models used in this research included: surface remesher, polyhedral mesher, and prism layer mesher.

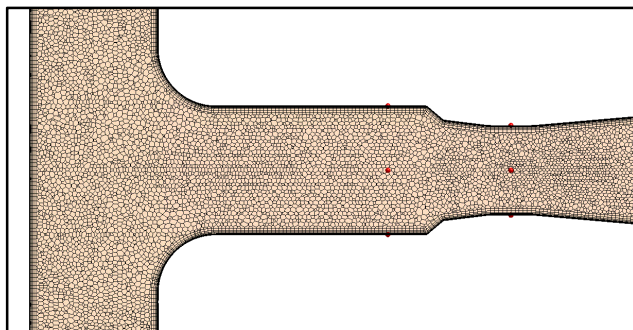


Fig. 6 Mesh of the 6-inch UVT meter at 0D

The uncertainty in the numerical results were determined by following a procedure published by

the ASME Journal of Fluids Engineering [10]. The study states that three meshes be used with cell sizes that are at least 1.3 times greater than the following mesh. Using this procedure, a Grid convergence index (GCI) was determined for a 6-in UVT, 24-in classical Venturi, and a 48-in classical Venturi, for which the GCI for discretization error did not exceed 0.05% (Table II).

TABLE III
GCI FOR THREE NUMERICAL RUNS

Grid Convergence Index Runs			
Parameter	6-inch	24-inch	48-inch
R_{21}	1.40	1.43	1.43
R_{32}	1.44	1.50	1.50
R_{43}			
ϕ_1	0.9585	0.9888	0.9878
ϕ_2	0.9579	0.9908	0.9900
ϕ_3	0.9546	0.9907	0.9904
ϕ_4			
P	4.7	9.1	5.3
Q(p)	-0.18	-0.43	-0.30
S	1	-1	1
ϕ_{ext}^{21}	1	1	1
ϕ_{ext}^{32}			
e_a^{21}	0.059%	0.198%	0.226%
e_{ext}^{21}	0.015%	0.008%	0.041%
GCI_{fine}^{21}	0.02%	0.01%	0.05%

IV. RESULTS

Plots comparing numerical and physical results were used to illustrate the performance of the Venturi meter downstream of the tee junction. The plots compared percent deviation (tee discharge coefficient to the straight-line discharge coefficient) to the Reynolds number passing through the Venturi meter. Each plot illustrates how the installation effects the discharge coefficient and consequently the flow measurement.

In order to verify the physical data, the 6-inch UVT was modelled first in CFD. Figure 7 shows

the straight-line calibration for both the physical results and CFD results. CFD yielded approximately a -2% shift from the physical, with the exception of the lower Reynolds numbers of the physical data. While the absolute difference between physical data and CFD data is interesting, the reader is once again reminded that the ability of CFD to identify differences in configurations is its real strength. The intent of the data for Figure 7 is to show how CFD does in absolutely predicting the actual discharge coefficient for the UVT meter. When one knows what the baseline value for the discharge coefficient is, either from the manufacturer or a laboratory calibration, adjustments may be made to improve measurement performance.

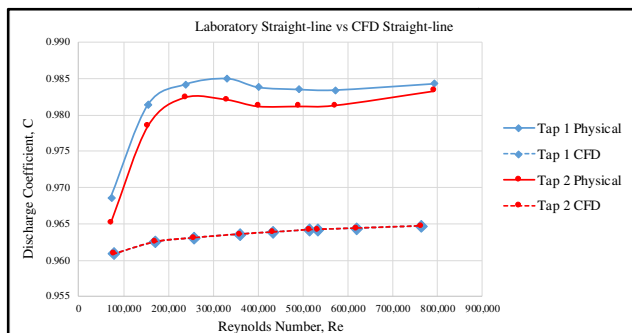


Fig. 7 Straight-line discharge coefficient for tap sets 1 and 2

Figure 8 shows the laboratory results with the CFD simulations for the four tap sets at 0D, while Figure 9 shows the results for the 5D installation. The percent deviation was calculated using interpolation for the straight-line C values to ensure the Reynolds numbers were the same at each flow split. From the figures, it becomes apparent that CFD models the physical trends better in tap sets three and four than in tap sets one and two. From Figure 9, it should be stressed that the CFD results for flow split four of tap set two and flow split one of tap set one do not adequately follow the physical trend at the lower Reynolds number. This is significant because if one were to use the CFD results for these configurations to adjust the given discharge coefficient, their solution would actually

be more incorrect than if they were to do nothing and simply use the given discharge coefficient. Therefore, these configurations should be avoided. It should be noted that the highest deviation at any flow split of CFD to physical was 1.7% for 0D and 1.9% for 5D for all tap sets.

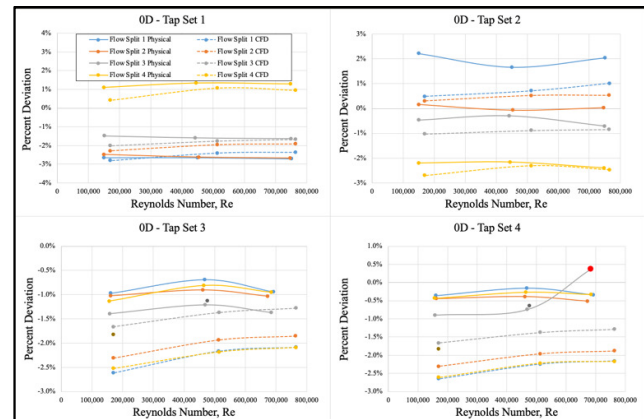


Fig. 8 Physical and CFD results for all tap sets at 0D. The red dot seen in the tap set four graph illustrates an outlier in the physical data

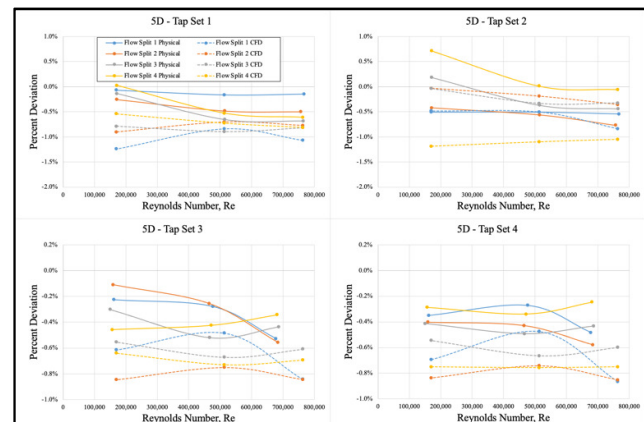


Fig. 9 Physical and CFD results for all tap sets at 5D

Figures 10 and 11 show the laboratory results with the CFD simulations for the four flow splits at 0D and 5D, respectively. From Figure 10, the overall trends are that as the flows from the converging lines approach a 50/50 split the percent deviation between tap sets decrease. This results in a smaller variation between laboratory and CFD data at flow split three than at flow splits one, two,

and four. From Figure 11, the CFD data models the physical data with little deviation between taps sets. However, CFD struggles to replicate the physical trends with the exception of flow split three. The CFD results for flow split three closely follow the physical trends and yields a maximum deviation from physical data of 0.65% across all tap sets.

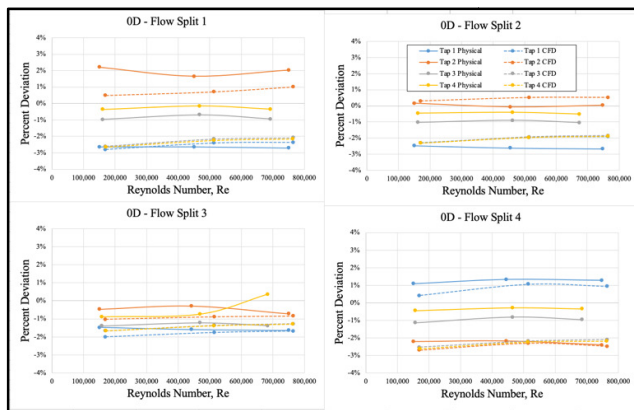


Fig. 10 Physical and CFD results for all four splits at 0D

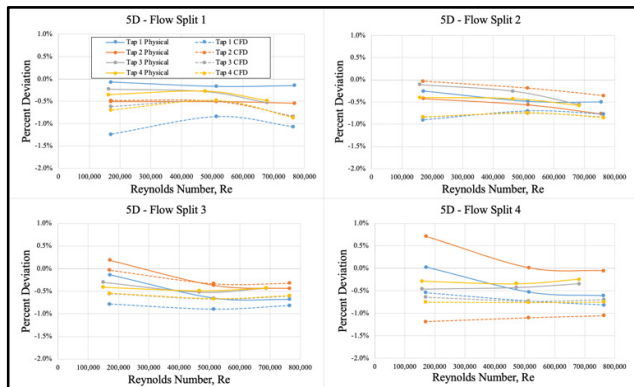


Fig. 11 Physical and CFD results for all four splits at 5D

As expected, the 0D installation was more difficult for CFD to model than the 5D installation. However, CFD still proved capable in modelling the physical trends at tap sets three and four, which allows for corrections to be made for the differences between CFD and physical data. The tap sets at 5D all performed well with the highest difference in percent deviation from physical to CFD being 1.17%, 1.90%, 0.73%, and 0.5% for tap

sets one, two, three, and four respectively. Along with having the smallest differences in deviation from the physical data, tap sets three and four modelled the physical trends better than tap sets one and two at 5D as well.

Figures 12 and 13 show the flow profiles at the meter's inlet for each of the flow splits along with a 50/50 and straight-line test at the same Reynolds number for both 0D and 5D. Flow split three (60/40) consistently outperforms the other flow splits because the flow profile entering the meter's inlet is comparatively more uniform. While the 50/50 flow split was not modelled in the laboratory, it can be assumed, based on the trends seen in Figures 10, 11, 12, and 13, that the 50/50 flow split would have a smaller percent deviation than the other flow splits.

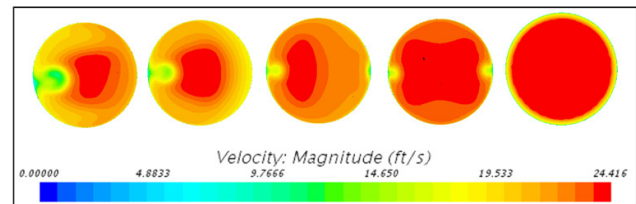


Fig. 12 Flow profiles of Venturi meter's inlet for flow splits at 0D. From left to right: 100/0, 80/20, 60/40, 50/50, straight-line

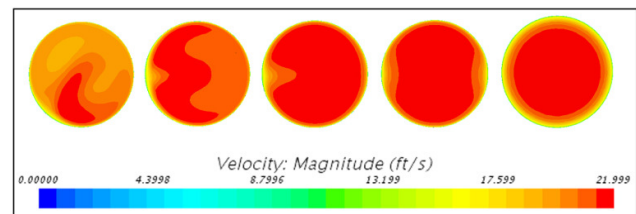


Fig. 13 Flow profiles of Venturi meter's inlet for flow splits at 5D. From left to right: 100/0, 80/20, 60/40, 50/50, straight-line

Additional CFD models were included in this study to understand the variables that influence the CFD results. One of the additional models changed the beta ratio in the UVT from 0.7 to 0.5. Figure 14 plots the percent deviation of this model against the 0.7 beta CFD data. The 0.5 beta UVT had an overall lower percent deviation from the straight-line calibration than the 0.7 beta UVT at 5D. The author concluded that the larger beta ratio is more susceptible to the upstream disturbance because the

larger throat area allowed for more pressure variation in the flow profile and therefore yielded a larger deviation.

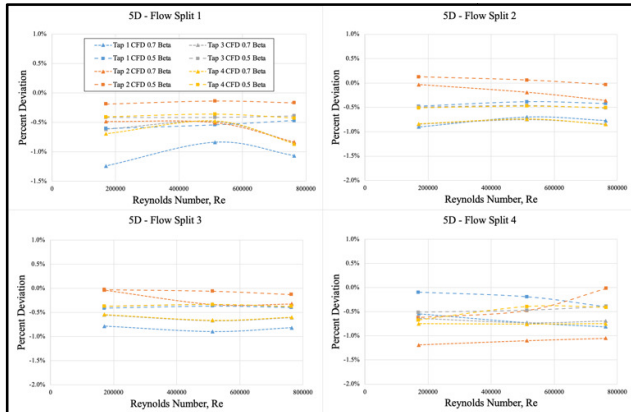


Fig. 14 CFD flow split results of 0.5 and 0.7 beta UVT at 5D

The other additional model changed the geometry of the tee junction from a rounded tee to a sharp-cornered tee. Figure 15 plots the percent deviation of this model against the rounded tee CFD data. The overall trend for flow splits one, two, and four is the sharp-cornered CFD results have a higher percent deviation and are more linear with few exceptions. Flow split three shows minor differences between the rounded and sharp-cornered tee, with the exception that the rounded tee approaches zero at the lower Reynolds number while the sharp-cornered tee slightly diverged.

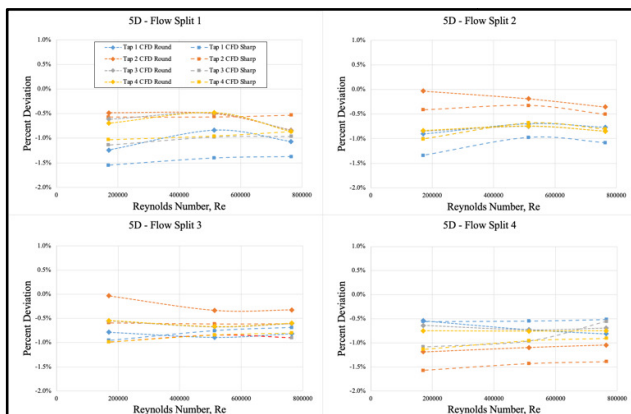


Fig. 15 CFD flow split results for round- and sharp-cornered tee at 5D

In addition to the sharp-cornered tee and 0.5 beta simulations, a series of 6-inch, 24-inch, and 48-inch simulations were also conducted to understand how pipe size influences the CFD results. The 6-, 24-, and 48-inch classical Venturi geometries followed the ASME PTC 19.5-2004 standard with a beta ratio of 0.5 and a converging cone half angle of 10.5 degrees and a diverging cone half angle of 7.5 degrees [11]. Figure 16 shows the CFD data for the 6-, 24-, and 48-inch simulations plotted against percent deviation and the Reynolds number. A range of Reynolds numbers were chosen to help illustrate how pipe size influences the CFD results. Figure 16 shows that the differences in the results between the three pipe diameters are insignificant, therefore, the author concluded no size scale effects exist from the numerical model.

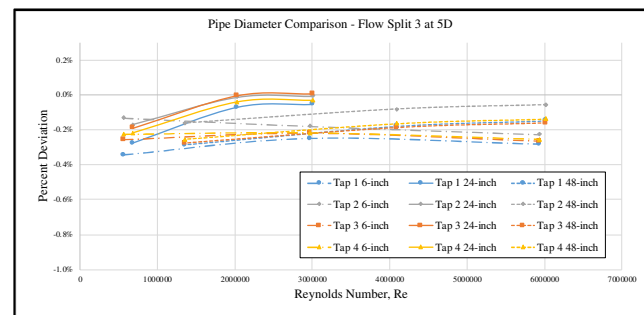


Fig. 16 Classical Venturi 24-inch diameter vs 48-inch diameter

The results of this study were used to develop contour plots that help to apply a correction factor to the manufacture's assigned discharge coefficient to decrease uncertainty in flow measurement. An example using a contour plot created from the CFD 6-inch OD data is provided in the following section.

V. EXAMPLE

A 6-inch UVT meter, with a 0.7 beta ratio, is installed close coupled (OD) to the branch of a tee junction with converging run flow. The UVT meter is rotated out of plane and has a given straight-line discharge coefficient of 0.9850. It is known that one of the converging flows has a Reynolds number of 2.5×10^5 , a fluid density of $\rho_f = 62.42 \text{ lb/ft}^3$, and a kinematic viscosity of $\nu = 1.931 \times 10^{-5} \text{ ft}^2/\text{s}$. With

the meter rotated out of plane, tap set three (top of pipe) produces a differential pressure of $\Delta P = 10.2$ psi. It is desired to have the known converging flow to be 30% of the total flow. To solve for the actual flow split, the 30% desired flow split will be used as a guess to begin the iterative process.

Solution: First, calculate the Venturi Reynolds number (total flow).

$$Re_{meter} = \frac{Re_{branch}}{30\%} = \frac{2.5 * 10^5}{0.30} = 0.83 * 10^6$$

Using the flow split and calculated Reynolds number, a correction coefficient ($C/C_{straight}$) can be derived from Figure 17. With a flow split of 0.3 and a Reynolds number of 0.83×10^6 , the $C/C_{straight}$ is roughly 0.9840.

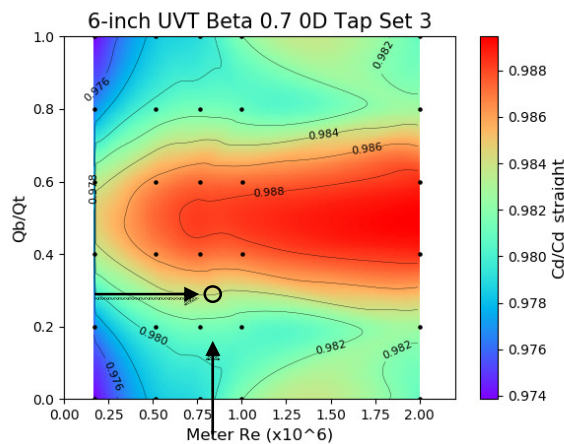


Fig. 17 Contour plot for tap set three of the 6-inch 0.7 beta UVT at OD

The given discharge coefficient can then be adjusted using the correction coefficient.

$$\frac{C}{C_{straight}} * C_{straight}(given) = 0.9840 * 0.9850 = 0.9692$$

Convert the differential pressure from psi to psf.

$$\Delta P = 10.2 \frac{lb}{in^2} * 144 \frac{in^2}{ft^2} = 1468.80 \frac{lb}{ft^2}$$

Calculate the area of the throat section of the UVT.

$$A_t = \frac{\pi}{4} * \left(\frac{6 * 0.7}{12} \right)^2 = 0.0962 ft^2$$

Calculate the flow rate, Q, using the Venturi equation (equation 1).

$$Q = 0.9692 * 0.0962 * \sqrt{\frac{2 * 32.2 * 1468.80}{(1 - 0.7^4) * 62.42}} = 4.16 \frac{ft^3}{s}$$

Calculate the adjusted Reynolds number using the flow rate just found.

$$Re_{meter} = \frac{VD}{\nu} = \frac{4.16 * \left(\frac{6}{12} \right)}{\left(\frac{\pi}{4} * \left(\frac{6}{12} \right)^2 \right) * 1.931 * 10^{-5}} = 0.55 * 10^6$$

Calculate the new flow split using the meter Reynolds number just calculated and the known branch Reynolds number.

$$Flow\ split = \frac{0.25 * 10^6}{0.55 * 10^6} * 100 = 45.52\%$$

The solution process now becomes iterative by finding a new correction coefficient using the calculated flow split and meter Reynolds number. Within three iterations the solution converged to a flow split of 45.38% with the last iteration changing the flow split by just 0.01%. With the desired flow split being 30%, the process would be repeated after having adjusted the control valves. For this example, the solution was considered converged once the solution changed by 0.02% or less.

If the flow rate were to be calculated for this example with the given C (0.985) the flow rate would be 4.23 cfs. The percent difference between

the flow rates of the adjusted discharge coefficient and the straight-line discharge coefficient is 1.3%. The percent difference provides insight into the importance of flow calibration and why a straight-line discharge coefficient is not suitable for an installation with disturbed flow conditions. As the flow split approaches a ratio of 100/0, it is expected that the percent difference would increase. Likewise, it is expected the percent difference would increase as the total flow decreases.

VI. CONCLUSION

Venturi meters are one of the most widely used flow measurement devices throughout the world and are commonly installed in undesirable conditions. When this occurs, a laboratory calibration would provide an adjusted discharge coefficient that properly represents the disturbed pressure profile. However, when laboratory modelling is not feasible or possible, this research is significant in that it provides readers with a method to adjust a Venturi meter's discharge coefficient for a Venturi that will be, or already is, installed on the branch of a tee junction with converging run flow.

VII. SYMBOLOGY

0D = Zero-diameters downstream of tee junction

5D = Five-diameters downstream of tee junction

C = Venturi discharge coefficient

$C_{straight}$ = Straight-line discharge coefficient

Q = Total flow rate (lb/s)

Y = Gas expansion coefficient

D = Venturi inlet diameter (ft)

d = Venturi throat diameter (ft)

g = Acceleration due to gravity (ft/s²)

ΔP = Differential pressure between the inlet taps

and throat taps (lb/ft²)

β = Beta ratio

ρ_f = Density of water (lb/ft³)

Re = Reynolds number

A_t = Throat area of Venturi meter

REFERENCES

- [1] The American Society of Mechanical Engineers (ASME), comp. *Addenda to ASME MFC-3M-2004: Measurement of Fluid Flow in Pipes Using Orifice, Nozzle, and Venturi*. March 24, 2008. ASME code, Three Park Avenue, New York. pp.75
- [2] Costa, N.P., Maia, R., Proenca, M. F. and Pinho, F. T. 2006. *Edge Effects on the Flow Characteristics in a 90 deg Tee Junction*. November 2006. ASME. *J. Fluids Eng.* 128(6): 1204-1217
- [3] Abdulwahhab, M., Injeti, N.K., Dakhil, S.F., *Numerical Prediction of Pressure Loss of Fluid in a T-Junction*. 2013. Journal of Energy and Environment. Vol. 4, No. 2.
- [4] Sharp, Z.B., Johnson, M.C., Barfuss, S.L., and Rahmeyer, W.J. 2009. *Energy Losses in Cross Junctions*. Journal of Hydraulic Engineering, Vol. 136, No. 1, January 2010.
- [5] Stauffer, T., Johnson, M.C., Barfuss, S.L., and Sorensen, A.D., *Hydraulic Average of Multiple Tap Sets to Improve Performance of Venturi Flowmeters with Upstream Disturbance*. 2019. All Graduate Theses and Dissertations. 7487.
- [6] Sandberg, Benjamin G., *Venturi Flowmeter Performance Installed Downstream of the Branch of a Tee Junction*. 2020. *All Graduate Theses and Dissertations*. 7825.
- [7] Day, Matthew P., *Classical Venturi Meter Performance Downstream of a Bifurcating Tee Junction*. 2022. International Journal of Scientific Research and Engineering Development. Vol. 5, No. 2: 339-348
- [8] The American Society of Mechanical Engineers (ASME), *Test uncertainty: An American national standard*. 2006. ASME PTC 19.1-2005, New York.
- [9] Sharp, Z.B., 2016. *Applications of Computational Fluid Dynamics in Flow Measurement and Meter Design*. Doctoral dissertation, Utah State University, Logan, Utah.
- [10] Celik, I.B., Ghia, U., Roache, P.J., Freitas, C.J., Coleman, H., and Raad, P.E. (2008). *Procedure for Estimation and Reporting of Uncertainty Due to Discretization in CFD Applications*. Journal of Fluids Engineering-Transactions of the ASME, 130, 078001-3.
- [11] The American Society of Mechanical Engineers (ASME), *Flow Measurement, Performance Test Codes*. 2004. ASME PTC 19.5-2004, New York. pp. 49-52